Circularly polarized-thermally activated delayed fluorescent materials based on chiral bicarbazole donors

Laurelie Poulard, Sitthichok Kasemthaveechok, Max Coehlo, Ramar Arun Kumar, Lucas Frederic, Patthira Sumsalee, Timothee d'Anfray, Sen Wu, Jingxiang Wang, Tomas Matulaitis, et al.

ChemComm

COMMUNICATION

View Article Online
View Journal | View Issue

Cite this: *Chem. Commun.*, 2022, **58**, 6554

Received 17th February 2022,
Accepted 4th May 2022

DOI: 10.1039/d2cc00998f

rsc.li/chemcomm

Circularly polarized-thermally activated delayed fluorescent materials based on chiral bicarbazole donors†

Laurélie Poulard,[a] Sitthichok Kasemthaveechok,[b] Max Coehlo,[a] Ramar Arun Kumar,[ac] Lucas Frédéric,[a] Patthira Sumsalee,[b] Timothée d'Anfray,[a] Sen Wu,[d] Jingxiang Wang,[d] Tomas Matulaitis,[d] Jeanne Crassous,[b] Eli Zysman-Colman,[d] Ludovic Favereau *[b] and Grégory Pieters *[a]

We describe herein a molecular design to generate circularly polarized thermally activated delayed fluorescence emitters in which chiral bicarbazole donors are connected to acceptor units *via* a rigid 8-membered cycle and how the nature of the donor and acceptor units affect the photophysical and chiroptical properties.

The design of circularly polarized (CP) emitters has recently attracted significant attention owing to the potential to exploit CP-light in different domains, ranging from chiroptoelectronics such as CP-organic light-emitting diodes (CP-OLEDs) and optical information processing, to bio-imaging or chiral sensing.[1] In this context and despite their theoretically low luminescence dissymmetry factors, g_{lum}, chiral organic luminophores have emerged into the spotlight. This interest is notably due to the ease with which their optoelectronic properties can be tuned and how processable they are compared to chiral lanthanoid and transition metal-based complexes.[2] In particular, the development of molecular designs merging CP luminescence and thermally activated delayed fluorescence (TADF) has evoked strong interest due to the potential of these materials to enhance the efficiency of OLED displays.[3] Currently, two main strategies have been investigated in the design of CP-TADF emitters based on either: (i) inherently chiral TADF chromophore, in which the chiral element is electronically involved in the emissive excited state[4] or; (ii) the use of a peripheral chiral element that is not directly involved in the emissive excited state but is essential to induce the chiroptical properties.[5] Following this second approach, some of us have pioneered the design of CP-TADF emitters using BINOL as a chiral perturbation unit (Fig. 1).[5b,f] This design has been largely employed to develop CP-TADF molecules displaying promising chiroptical properties, with g_{lum} reaching 2.0×10^{-3} in solution,[5b] or integrated within CP-OLEDs with high external quantum efficiency.[5c] Nevertheless, designing inherently chiral TADF emitters remains the strategy of choice for reaching high intensity of chiroptical properties, as highlighted by the recent works from the Chen group who showed that using a biaryl atropisomer acceptor with carbazole donor units afforded an emitter with $g_{lum} = 5.0 \times 10^{-3}$ in toluene solution (Fig. 1, top middle).[4d,e]

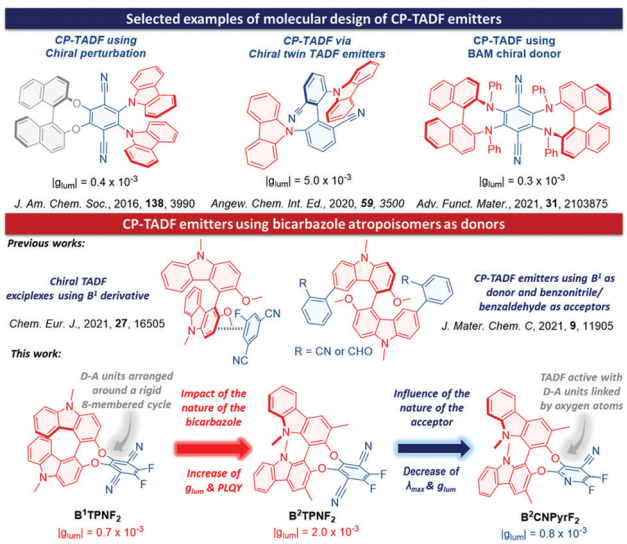

Fig. 1 Top: Selected molecular designs of reported CP-TADF emitters, and bottom: structures of the reported CP-TADF emitters based on bicarbazole atropoisomers compared to the ones described in this work.

[a] *Université Paris-Saclay, CEA, INRAE, Département Médicaments et Technologies pour la Santé (DMTS), SCBM, 91191 Gif-sur-Yvette, France. E-mail: gregory.pieters@cea.fr*
[b] *Univ Rennes, CNRS, ISCR-UMR 6226, ScanMAT-UMS 2001, F-35000 Rennes, France. E-mail: ludovic.favereau@univ-rennes1.fr*
[c] *SRM Research Institute, Department of Chemistry, SRM Institute of Science and Technology, Kattankulathur, 603203 Chennai, Tamilnadu, India*
[d] *Organic Semiconductor Centre, EaStCHEM School of Chemistry, University of St. Andrews, St. Andrews, Fife, KY16 9ST, UK*

† Electronic supplementary information (ESI) available: Synthetic protocols, spectra and computational details. See DOI: https://doi.org/10.1039/d2cc00998f

In line with the recent results of Zhou, Zheng and Zuo *et al.*, who reported the use of chiral donor *N*,*N*′-diphenyl-[1,1′-binaphthalene]-2,2′-diamine (BAM, Fig. 1),[4c] we surmised that chiral bicarbazole units within rigid donor–acceptor systems may result in an alternative molecular design to merge CPL and TADF properties. In this context, 9,9′-dimethyl-9*H*,9′*H*-[4,4′-bicarbazole]-3,3′-diol (**B^1**) derivatives have been used to develop the first TADF exciplexes and to synthesize axial/helical TADF emitters displaying interesting modulation of their chiroptical properties depending on the solvent polarity (Fig. 1 bottom).[5] In this communication, we report the synthesis, photophysical and chiroptical properties of three chiral emitters, **B^{1}TPNF$_2$**, **B^{2}TPNF$_2$** and **B^{2}CNPyrF$_2$**, containing C_2-symmetric bicarbazole (**B^1** and 3,3′,9,9′-tetramethyl-9*H*,9′*H*-[1,1′-bicarbazole]-2,2′-diol (**B^2**)) electron-donor systems that are coupled with either difluoroterephthalonitrile or difluorocyanopyridine as electron-accepting units. These compounds display CP-TADF with $|g_{lum}|$ values up to 2.0×10^{-3} and very small singlet triplet energy gaps (ΔE_{ST}). In terms of molecular design, the chiral donor part and the acceptor units are connected *via* a rigid 8-membered cycle with oxygen atoms (Fig. 1), which is expected to facilitate the spatial separation of the frontier molecular orbitals. Interestingly, the nature of the bicarbazole isomer, at either the 1- or the 4-carbazole position, also strongly affects the photophysical and chiroptical properties of the compounds, with more than a two-fold difference of both the measured $|g_{lum}|$ and photoluminescence quantum yield (PLQY) values, providing new insights for the design of improved CP-TADF emitters.

We started our study by performing DFT calculations (M06-2X/6-311G(d,p) in DCM) to evaluate the degree of overlap between the highest occupied molecular orbital (HOMO) and the lowest unoccupied molecular orbital (LUMO) of each of **B^{1}TPNF$_2$**, **B^{2}TPNF$_2$** and **B^{2}CNPyrF$_2$**. As depicted in Fig. 2A, the three compounds show spatially well separated HOMO and LUMO, which are localized on the bicarbazole donor and the acceptor fragments, respectively. Such a weak frontier orbitals overlap is likely to induce small ΔE_{ST} in these molecules, which is of high importance to facilitate an efficient intersystem crossing and TADF activity.[7] The synthesis of the target compounds firstly involves the preparation of the two bicarbazole **B^1** and **B^2**, implying successively the formation of the carbazole fragment and a dimerization reaction at either the 1- or the 4-carbazole positions to afford both chiral donor units.[8] Whereas an optimized synthesis of **B^1** was recently reported,[6] the preparation of **B^2** has been revisited (Fig. 2B) in order to increase the overall yield of this promising chiral building block. This new route involves a Buchwald–Hartwig coupling reaction between **1** and **2** in 91% yield, followed by an intramolecular cyclization to afford **4** in 87% yield. After demethylation with BBr_3, **5** was engaged in an oxidative coupling reaction using $VO(acac)_2$ as the catalyst to afford **B^2**, in 61% yield. **B^{1}TPNF$_2$**, **B^{2}TPNF$_2$** and **B^{2}CNPyrF$_2$** were then each obtained through a nucleophilic aromatic substitution involving the corresponding bicarbazole derivatives and 2,3,5,6-tetrafluoroterephthalonitrile or 2,3,5,6-tetrafluoro-4-pyridinecarbonitrile as electrophiles. Preparative chiral supercritical fluid chromatography of **B^{2}TPNF$_2$** and **B^{2}CNPyrF$_2$** afforded the corresponding enantiomers, with ee up to 99% (Fig. S20 and S21, ESI†) while enantiomers of **B^{1}TPNF$_2$** were directly obtained using enantiopure (*R*) and (*S*)-**B^1** in the S_NAr reaction. The absorption spectra of the three molecules in dichloromethane (DCM) solution display a globally similar profile (Fig. S24–S26, ESI†), with two main bands in the higher energy part of the spectra (between 250–300 nm, $\varepsilon \sim 15.0$–40.0×10^3 M^{-1} cm^{-1}), and a lower energy set of bands between 320 and 360 nm ($\varepsilon \sim 5.0$–10.0×10^3 M^{-1} cm^{-1}). Both **B^{1}TPNF$_2$** and **B^{2}CNPyrF$_2$** display two distinguishable absorption bands at around 330 and 360 nm ($\varepsilon \sim 5.0$–10.0×10^3 M^{-1} cm^{-1}, Fig. 3), while **B^{2}TPNF$_2$** shows only one main band at 340 nm with a weak low energy broad tail that extends until 425 nm ($\varepsilon \sim 1.0 \times 10^3$ M^{-1} cm^{-1} at 400 nm). For each compound, these bands can be attributed to a mixture of bicarbazole-based π–π* locally excited (LE) and intramolecular charge transfer (ICT) transitions, namely from the bicarbazole unit to the difluoroterephthalonitrile or difluoro-4-pyridinecarbonitrile unit for the low energy band (Fig. S22–S26, ESI†). Further insight in the differences observed between the LE and ICT in the absorption spectra of the compounds can be further obtained by TD-DFT calculations (M06-2X/6-311G(d,p) in DCM, Fig. S59–S61 and S64, ESI†). While for **B^{2}TPNF$_2$**, the $S_{0\text{-}1}$ excitation can be assigned to an almost pure ICT character implying mainly the HOMO–LUMO

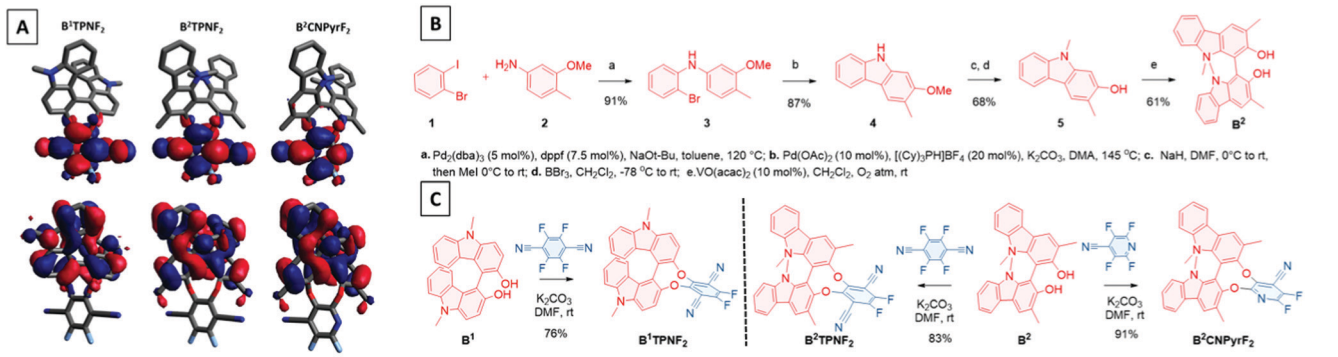

Fig. 2 (A) Isosurfaces (isovalue 0.02) of HOMO (bottom) and LUMO (top) for **B^{1}TPNF$_2$**, **B^{2}TPNF$_2$** and **B^{2}CNPyrF$_2$**; (B) new synthetic pathway developed for **B^2** and (C) synthesis of **B^{1}TPNF$_2$**, **B^{2}TPNF$_2$** and **B^{2}CNPyrF$_2$**.

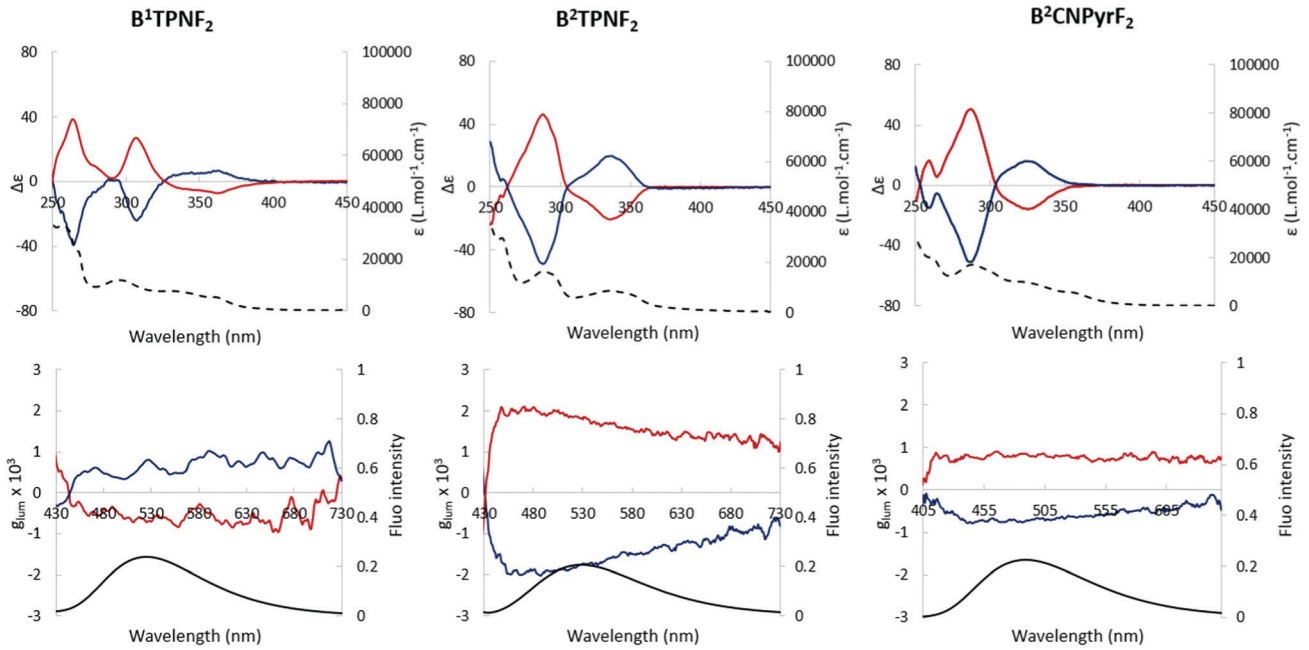

Fig. 3 Top: ECD and UV-vis (dashed line) spectra of **B¹TPNF₂**, **B²TPNF₂** and **B²CNPyrF₂** measured in DCM at 298 K (~10^{-5} M), and bottom: $g_{lum} = f(\lambda)$ curves in toluene ($C = 10^{-4}$ M) for **B¹TPNF₂**, **B²TPNF₂** and **B²CNPyrF₂** (blue and red lines for (*R*)- and (*S*)-enantiomers respectively).

transition (95%) with a minor LE contribution from the bicarbazole donor moiety (2%), the latter becomes more pronounced for both **B¹TPNF₂** and **B²CNPyrF₂**, decreasing the contribution of the HOMO−LUMO transition (90% and 81% for **B¹TPNF₂** and **B²CNPyrF₂**, respectively). **B¹TPNF₂** and **B²TPNF₂** can be considered as "donor–acceptor isomers", while **B²CNPyrF₂** bears a weaker electron acceptor **CNPyrF₂** but the same bicarbazole donor, thus it is expected that the three compounds will show a similar oxidation behaviour while **B²CNPyrF₂** will show a cathodically shifted reduction potential. While the electrochemical behaviour reveals an expected cathodically shifted reduction potential of −1.70 V for **B²CNPyrF₂** compared to *ca.* −1.40 V recorded for **B²TPNF₂** and **B¹TPNF₂**, the latter compound displays a 180 mV higher oxidation potential than the **B²** donor-based compounds (Fig. S33 and S34, ESI†), arising presumably from the relative *para*- and *meta*-connection of the oxygen atoms to the nitrogen ones on the carbazolyl moieties. The corresponding estimated HOMO and LUMO energies are −5.69/−2.99, −5.51/−2.88 and −5.55/−2.64 eV for **B¹TPNF**, **B²TPNF₂** and **B²CNPyrF₂**, respectively. Further differences between the two latter compounds are also clearly evidenced in their corresponding electronic circular dichroism (ECD) spectra (Fig. 3).

While (*S*)-**B¹TPNF₂** shows two positive signals at 270 and 305 nm ($\Delta\varepsilon \approx +35-40$ M^{-1} cm^{-1}), followed by a broader negative one in the low energy region ($\Delta\varepsilon \approx -5$ M^{-1} cm^{-1}), (*S*)-**B²TPNF₂** and (*S*)-**B²CNPyrF₂** display only positive and negative signals at 290 and 340 nm, respectively, associated with an overall higher intensity than the bands observed in **B¹TPNF₂**. This is notably illustrated by the calculated dissymmetry factor, g_{abs}, of $\pm 2.4 \times 10^{-3}$ for **B²TPNF₂** at 340 nm, $\pm 0.5 \times 10^{-3}$ for **B²CNPyrF₂** at 352 nm and of $\pm 1.1 \times 10^{-3}$ for **B¹TPNF₂** at 360 nm. We next investigated the emission properties of these chiral emitters in toluene solution. All of them show a broad luminescence, typical of a charge transfer emission process, with λ_{max} at 529, 530 nm and 492 nm for **B¹TPNF₂**, **B²TPNF₂** and **B²CNPyrF₂**, respectively (Fig. 3 and Fig. S30–S32, ESI†). The measured optical gaps, determined at the intersection of the normalized absorption and emission spectra, of 3.03, 2.94 and 2.86 eV for **B²CNPyrF₂**, **B¹TPNF₂** and **B²CNPyrF₂** fully confirm the trend observed in the UV-vis absorption spectra and electrochemistry measurements, with an expected impact of the electron accepting unit between **B²TPNF₂** and **B²CNPyrF₂**, and a noticeable

Table 1 Photophysical properties of the CP-TADF emitters

Compound	λ_{abs}[a] (nm)	λ_{em}[a] (nm)	PLQY[a] (air/Ar) in %	τ_{PL} (PF in ns/DF in μs)	ΔE_{ST}[c] (eV)	H/L[d] (eV)
B¹TPNF₂	363	529	5/11	10.1[a]/0.78[a]	0.00	−5.69/−2.99
B²TPNF₂	341	530[a]/527[b]	11/29	60.2[a] (69.4)[b]/0.953[a] (2.17)[b]	0.00	−5.51/−2.88
B²CNPyrF₂	358	492[a]/488[b]	9/23	49.0[a] (54.1)[b]/0.569[a] (1.84)[b]	0.22	−5.55/−2.64

[a] Measured in toluene solutions. [b] In 1 wt% doped mCP films (λ_{exc} = 379 nm). [c] In 2-MeTHF glass at 77 K (λ_{exc} = 360 nm). [d] Measured by CV (in DCM).

effect of the bicarbazole donor on the CT character of the low energy transition between $\mathbf{B^2TPNF_2}$ and $\mathbf{B^1TPNF_2}$. The three chiral emitters showed TADF, as evidenced by the bi-exponential decay recorded in degassed toluene solution, including the presence of a temperature-dependent sub-microsecond lifetime component (Table 1 and Fig. S35–S43, Table S1 for the rate constants, ESI†). Moreover, near-zero values of ΔE_{ST} were measured for $\mathbf{B^1TPNF_2}$ and $\mathbf{B^2TPNF_2}$, while that for $\mathbf{B^2CNPyrF_2}$ was slightly higher (0.22 eV) in 2-MeTHF glass at 77 K (Fig. S46–S48, ESI†). These experimental values were confirmed with theoretical calculations with calculated ΔE_{ST} of 0.02, 0.02 and 0.05 eV for $\mathbf{B^1TPNF_2}$, $\mathbf{B^2TPNF_2}$ and $\mathbf{B^2CNPyrF_2}$, respectively (PBE0/6-311G(d,p) level of theory, see Fig. S62, ESI†). Interestingly, $\mathbf{B^2TPNF_2}$ displays higher PLQYs both in aerated and degassed toluene solutions (0.11 and 0.29, respectively) than $\mathbf{B^1TPNF_2}$ (0.05 and 0.11), unambiguously highlighting the impact of the nature of the chiral donor on the photophysical properties. $\mathbf{B^2CNPyrF_2}$, bearing the same donor, possesses a similar PLQY value of 0.23 as that for $\mathbf{B^2TPNF_2}$. The obtained mirror-image CPL responses in toluene solutions display $|g_{lum}|$ of 0.7×10^{-3} for $\mathbf{B^1TPNF_2}$, 2.0×10^{-3} for $\mathbf{B^2TPNF_2}$, and 0.8×10^{-3} for $\mathbf{B^2CNPyrF_2}$, with similar maxima to their corresponding emission spectra. Theoretically, g_{lum} value can be approximated using the following formula $g_{lum} = 4 \cos\theta(\mu_m/\mu_e)$ where μ_e and μ_m are the electric and magnetic transition dipole moments (for the $S_{1\text{-}0}$ transition) respectively and θ, the angle between them. As suggested by the TD-DFT calculations (M06-2X/6-311G(d,p) in toluene, see ESI,† Page 56), the higher value of g_{lum} measured for $\mathbf{B^2TPNF_2}$ compared to $\mathbf{B^1TPNF_2}$ can be rationalized by a more favorable relative orientation of μ_m and μ_e whereas using $\mathbf{CNPyrF_2}$ as the acceptor has a detrimental impact both on the amplitude of μ_m and $\cos\theta$.

This communication reports a molecular design to generate CP-TADF emitters using axially chiral bicarbazoles as donor and terephthalonitrile or cyanopyridine as acceptor. In the context of TADF molecular design, these results show that the arrangement of donor and acceptor units, separated by oxygen atoms in a rigid 8-membered ring can resulted in a near-zero ΔE_{ST}. In terms of chiroptical and photophysical properties, the use of $\mathbf{B^2}$ as chiral donor was found to be beneficial and the origin of these enhancements have been explained by TD-DFT calculations. These results further highlight the importance of structure/properties relationship studies to guide the design of CPL emitters and may help to establish new molecular guidelines for the design of more efficient (CP-)TADF emitters.

L. P., S. K., M. C., R. A. K., L. F.: synthesis and characterisation; P. S., S.W.; J. W., T. M., E. Z.-C.: photophysical characterisation, DFT calculations, manuscript writing; T. D.'A: SFC purification; J. C., L. Fa., G. P. DFT calculations, direction of investigations, manuscript writing.

G. P. thanks the SCBM, the "PTC du CEA" (POLEM) and the ANR (iChiralight, ANR-19-CE07-0040) for funding and David Buisson, Amélie Goudet and Sabrina Lebrequier. J. C. and L. Fa. acknowledge the Ministère de l'Education Nationale, de la Recherche et de la Technologie, the CNRS and the Spectroscopies-CDTP core facility is also acknowledged. The St. Andrews team thanks the China Scholarship Council, 201906250199 to W. S. and 202006250026 to J. W., E. Z.-C. is a Royal Society Leverhulme Trust Senior Research fellow (SRF\R1\201089). We thank the EPSRC (EP/R035164/1) for funding.

Conflicts of interest

Patent pending PCT/EP2021/069232.

Notes and references

1 (*a*) R. Carr, N. H. Evans and D. Parker, *Chem. Soc. Rev.*, 2012, **41**, 7673–7686; (*b*) L. E. MacKenzie and R. Pal, *Nat. Rev. Chem.*, 2021, **5**, 109–124; (*c*) Y. Sang, J. Han, T. Zhao, P. Duan and M. Liu, *Adv. Mater.*, 2020, **32**, 1900110; (*d*) J. R. Brandt, F. Salerno and M. J. Fuchter, *Nat. Rev. Chem.*, 2017, **1**, 0045.

2 (*a*) E. M. Sánchez-Carnerero, A. R. Agarrabeitia, F. Moreno, B. L. Maroto, G. Muller, M. J. Ortiz and S. de la Moya, *Chem. – Eur. J.*, 2015, **21**, 13488–13500; (*b*) H. Tanaka, Y. Inoue and T. Mori, *ChemPhotoChem*, 2018, **2**, 386–402; (*c*) L. Arrico, L. Di Bari and F. Zinna, *Chem. – Eur. J.*, 2021, **9**, 2920–2934.

3 (*a*) L. Frédéric, A. Desmarchelier, L. Favereau and G. Pieters, *Adv. Funct. Mater.*, 2021, **31**, 2010281; (*b*) D.-W. Zhang, M. Li and C.-F. Chen, *Chem. Soc. Rev.*, 2020, **49**, 1331–1343.

4 For recent selected examples see: (*a*) X. Wu, J.-W. Huang, B.-K. Su, S. Wang, L. Yuan, W.-Q. Zheng, H. Zhang, Y.-X. Zheng, W. Zhu and P.-T. Chou, *Adv. Mater.*, 2022, **34**, 2105080; (*b*) S.-Y. Yang, S.-N. Zou, F.-C. Kong, X.-J. Liao, Y.-K. Qu, Z.-Q. Feng, Y.-X. Zheng, Z.-Q. Jiang and L.-S. Liao, *Chem. Commun.*, 2021, **57**, 11041–11044; (*c*) Z. P. Yan, T. T. Liu, R. Wu, X. Liang, Z. Q. Li, L. Zhou, Y. X. Zheng and J. L. Zuo, *Adv. Funct. Mater.*, 2021, **31**, 2103875; (*d*) M. Li, Y. F. Wang, D. Zhang, L. Duan and C. F. Chen, *Angew. Chem., Int. Ed.*, 2020, **59**, 3500–3504; (*e*) Y. F. Wang, M. Li, W. L. Zhao, Y. F. Shen, H. Y. Lu and C. F. Chen, *Chem. Commun.*, 2020, **56**, 9380–9383; (*f*) S. Y. Yang, Y. K. Wang, C. C. Peng, Z. G. Wu, S. Yuan, Y. J. Yu, H. Li, T. T. Wang, H. C. Li, Y. X. Zheng, Z. Q. Jiang and L. S. Liao, *J. Am. Chem. Soc.*, 2020, **142**, 17756–17765; N. Sharma, E. Spuling, C. M. Mattern, W. Li, O. Fuhr, Y. Tsuchiya, C. Adachi, S. Bräse, I. D.-W. Samuel and E. Zysman-Colman, *Chem. Sci.*, 2019, **10**, 6689–6696.

5 (*a*) Y. Xu, Q. Wang, X. Cai, C. Li and Y. Wang, *Adv. Mater.*, 2021, **33**, 2100652; (*b*) L. Frédéric, A. Desmarchelier, R. Plais, L. Lavnevich, G. Muller, C. Villafuerte, G. Clavier, E. Quesnel, B. Racine, S. Meunier-Della-Gatta, J. P. Dognon, P. Thuéry, J. Crassous, L. Favereau and G. Pieters, *Adv. Funct. Mater.*, 2020, **30**, 2004838; (*c*) Z. G. Wu, H. B. Han, Z. P. Yan, X. F. Luo, Y. Wang, Y. X. Zheng, J. L. Zuo and Y. Pan, *Adv. Mater.*, 2019, **31**, 1900524; (*d*) Z.-G. Wu, Z.-P. Yan, X.-F. Luo, L. Yuan, W.-Q. Liang, Y. Wang, Y.-X. Zheng, J.-L. Zuo and Y. Pan, *J. Mater. Chem. C*, 2019, **7**, 7045–7052; (*e*) F. Song, Z. Xu, Q. Zhang, Z. Zhao, H. Zhang, W. Zhao, Z. Qiu, C. Qi, H. Zhang, H. H.-Y. Sung, I. D. Williams, J. W.-Y. Lam, Z. Zhao, A. Qin, D. Ma and B. Z. Tang, *Adv. Funct. Mater.*, 2018, **28**, 1800051; (*f*) S. Feuillastre, M. Pauton, L. Gao, A. Desmarchelier, A. J. Riives, D. Prim, D. Tondelier, B. Geffroy, G. Muller, G. Clavier and G. Pieters, *J. Am. Chem. Soc.*, 2016, **138**, 3990–3993.

6 (*a*) S. Kasemthaveechok, L. Abella, M. Jean, M. Cordier, T. Roisnel, N. Vanthuyne, T. Guizouarn, O. Cador, J. Autschbach, J. Crassous and L. Favereau, *J. Am. Chem. Soc.*, 2020, **142**, 20409–20418; (*b*) P. Sumsalee, L. Abella, T. Roisnel, S. Lebrequier, G. Pieters, J. Autschbach, J. Crassous and L. Favereau, *J. Mater. Chem. C*, 2021, **9**, 11905–11914; (*c*) P. Sumsalee, L. Abella, S. Kasemthaveechok, N. Vanthuyne, M. Cordier, G. Pieters, J. Autschbach, J. Crassous and L. Favereau, *Chem. – Eur. J.*, 2021, **27**, 16505–16511.

7 (*a*) M. Y. Wong and E. Zysman-Colman, *Adv. Mater.*, 2017, **29**, 1605444; (*b*) Z. Yang, Z. Mao, Z. Xie, Y. Zhang, S. Liu, J. Zhao, J. Xu, Z. Chi and M. P. Aldred, *Chem. Soc. Rev.*, 2017, **46**, 915–1016.

8 (*a*) P. N.-M. Botman, M. Postma, J. Fraanje, K. Goubitz, H. Schenk, J. H.-V. Maarseveen and H. Hiemstra, *Eur. J. Org. Chem.*, 2002, 1952–1955; (*b*) M. Sako, K. Higashida, G. T. Kamble, K. Kaut, A. Kumar, Y. Hirose, D.-Y. Zhou, T. Suzuki, M. Rueping, T. Maegawa, S. Takizawa and H. Sasai, *Org. Chem. Front.*, 2021, **8**, 4878–4885; (*c*) L. Liu, P. J. Carroll and M. C. Kozlowski, *Org. Lett.*, 2015, **3**, 508–511.